On the Linearity of Local and Regional Temperature Changes from 1.5°C to 2°C of Global Warming

ANDREW D. KING,[a] RETO KNUTTI,[b] PETER UHE,[c] DANIEL M. MITCHELL,[c] SOPHIE C. LEWIS,[d] JULIE M. ARBLASTER,[e] NICOLAS FREYCHET[f]

[a] *Australian Research Council Centre of Excellence for Climate Extremes, School of Earth Sciences, University of Melbourne, Melbourne, Victoria, Australia*
[b] *Institute for Atmospheric and Climate Science, ETH Zurich, Zurich, Switzerland*
[c] *School of Geographical Sciences, University of Bristol, Bristol, United Kingdom*
[d] *School of Physical Environmental and Mathematical Sciences, University of New South Wales, Canberra, Australian Capital Territory, Australia*
[e] *Australian Research Council Centre of Excellence for Climate Extremes, School of Earth, Atmosphere and Environment, Monash University, Melbourne, Australia, and National Center for Atmospheric Research, Boulder, Colorado*
[f] *School of Geosciences, University of Edinburgh, Edinburgh, United Kingdom.*

(Manuscript received 29 September 2017, in final form 1 June 2018)

ABSTRACT

Given the Paris Agreement it is imperative there is greater understanding of the consequences of limiting global warming to the target 1.5° and 2°C levels above preindustrial conditions. It is challenging to quantify changes across a small increment of global warming, so a pattern-scaling approach may be considered. Here we investigate the validity of such an approach by comprehensively examining how well local temperatures and warming trends in a 1.5°C world predict local temperatures at global warming of 2°C. Ensembles of transient coupled climate simulations from multiple models under different scenarios were compared and individual model responses were analyzed. For many places, the multimodel forced response of seasonal-average temperatures is approximately linear with global warming between 1.5° and 2°C. However, individual model results vary and large contributions from nonlinear changes in unforced variability or the forced response cannot be ruled out. In some regions, such as East Asia, models simulate substantially greater warming than is expected from linear scaling. Examining East Asia during boreal summer, we find that increased warming in the simulated 2°C world relative to scaling up from 1.5°C is related to reduced anthropogenic aerosol emissions. Our findings suggest that, where forcings other than those due to greenhouse gas emissions change, the warming experienced in a 1.5°C world is a poor predictor for local climate at 2°C of global warming. In addition to the analysis of the linearity in the forced climate change signal, we find that natural variability remains a substantial contribution to uncertainty at these low-warming targets.

1. Introduction

The Paris Agreement of 2015 (UNFCCC 2015) has resulted in an international effort to limit global warming to well below 2°C above pre-industrial levels and to pursue efforts to limit the temperature increase to 1.5°C above pre-industrial levels. Consequently, there is a need for policymakers to receive scientific advice on the benefits of limiting global warming to 1.5°C relative to higher levels of warming such as 2°C (Schleussner et al. 2016; Mitchell et al. 2016b; James et al. 2017).

The Intergovernmental Panel on Climate Change is compiling a special report on ''global warming of 1.5°C'' to be published in 2018. To date, there have been several studies that have explored global and regional climatic changes at these levels (Schleussner et al. 2016; King and Karoly 2017; Lehner et al. 2017; Dosio and Fischer 2018), although further analysis is required.

Some studies have suggested that scaling temperature and precipitation changes between different levels of global warming provides a reasonable approximation for climate projections (Tebaldi and Arblaster 2014;

Supplemental information related to this paper is available at the Journals Online website: https://doi.org/10.1175/JCLI-D-17-0649.s1.

Corresponding author: Andrew King, andrew.king@unimelb.edu.au

DOI: 10.1175/JCLI-D-17-0649.1

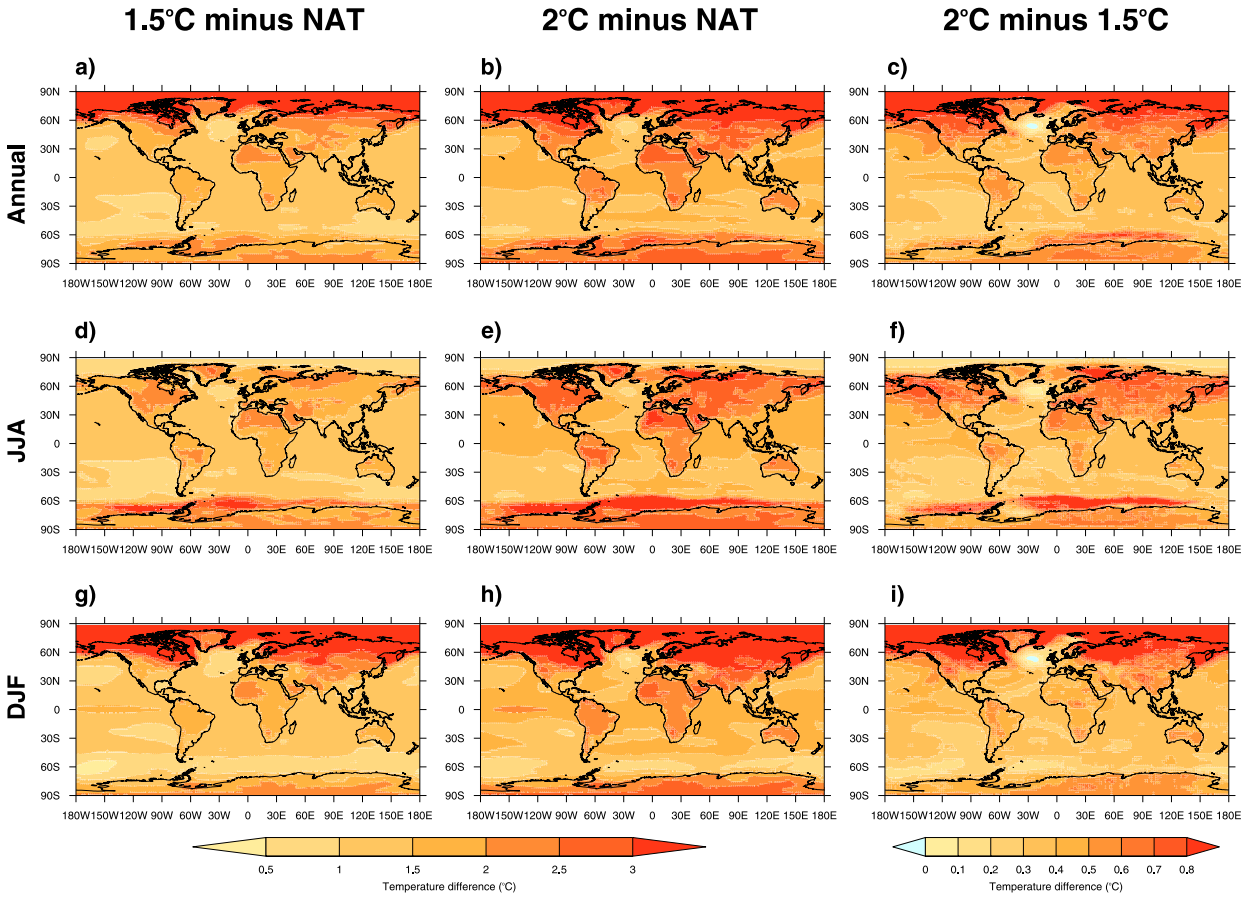

FIG. 1. Change in average (a)–(c) annual, (d)–(f) JJA, and (g)–(i) DJF model median temperature between (left) a natural climate and 1.5°C, (middle) a natural climate and 2°C, and (right) 1.5° and 2°C of global warming.

Herger et al. 2015; Seneviratne et al. 2016). Indeed, patterns of warming from a natural baseline to 1.5° and 2°C are very similar on the global scale (Fig. 1) with pattern correlations (Spearman's rank) in excess of 0.98 for the annual, boreal summer, and boreal winter temperature changes. However, these high pattern correlations are dominated by consistent large-scale warming patterns such as Arctic amplification and the increased warming over land relative to the ocean. As a result, significant local and regional departures from linear scaling might be missed from these global statistics. Good et al. (2015) show that nonlinear regional warming patterns are projected, albeit for very large amounts of warming associated with doubling and quadrupling in atmospheric carbon dioxide concentrations. Also, Good et al. (2016) found nonlinearities in the precipitation response at a regional scale up to 2°C of global warming. This study investigates departures from linear scaling in more detail at 1.5° and 2°C of global warming above preindustrial levels. This is the first study to comprehensively assess the linearity of the local climate response to global warming at the policy-relevant Paris Agreement targets.

A detailed analysis of the linearity of regional warming projections for small increments of global warming, and the adequacy of linear scaling methods as a result, is needed. It is vital that there is better understanding of where scaling provides a good approximation for climatic changes between global warming levels and where it may not be as suitable an approach to take and further analysis is required. Despite the large agreement in the patterns of warming at the global level, there may well be regions where linear scaling provides a poor approximation for the warming we might expect at 2°C of global warming. It is hypothesized that where there are substantial climate change–caused dynamical changes in the climate system, for example, in the Southern Hemisphere extratropical storm track (Kushner et al. 2001; Arblaster and Meehl 2006), then there may be nonlinear changes in temperature (Knutti et al. 2016). Also, shifting sea ice boundaries would be expected to result in nonlinear temperature responses.

Differences in non–greenhouse gas forcings between scenarios may impact the linearity of warming as well (Good et al. 2015).

This study uses model simulations from phase 5 of the Coupled Model Intercomparison Project (CMIP5; Taylor et al. 2012) to investigate regional temperature changes from 1.5° to 2°C global warming relative to a natural baseline. A simple linear scaling of the simulated warming from the natural baseline to 1.5°C is extended to 2°C to generate a ''scaled 2°C world.'' This scaled warming is then compared with the model-simulated temperature projections at 2°C. Statistical significance of projected warming departures from scaling and the levels of model agreement in departures from scaling are investigated. Different methods for assessing departures from scaling and model spread and agreement are analyzed. Differences between the multimodel response and variations between models, as well as the implications for changes in risks between 1.5° and 2°C levels of global warming, are also discussed.

The East Asia region is highlighted as an area where scaling provides a poor analogy for simulated warming beyond 1.5°C. The mechanisms for nonlinear warming in the CMIP5 projections are analyzed in more detail over East Asia during boreal summer (JJA). The implications of nonlinear warming for extreme summer temperatures are also analyzed using an event attribution framework (e.g., Lewis and Karoly 2013; King et al. 2015b) for the first time. Climate extremes have greater impacts than mean climate changes, so by investigating the effect of scaling departures on extreme events we seek to identify if there is a change in likelihood of a high-impact event due to nonlinear warming trends.

2. Data and methods

a. *Model and observational data*

Model simulations from 16 state-of-the-art global climate models within the CMIP5 archive were used for this analysis. Model fields of surface air temperature (tas) were used first in the calculation of four different scenarios:

- a ''natural world'' (defined using the period 1901–2005 in the historicalNat simulations),
- a ''current world'' (defined as 2006–26 in the RCP8.5 simulations),
- a ''1.5°C world'' (defined as years under all the RCP scenarios within decades when global-average temperatures are between 1.3° and 1.7°C warmer than the corresponding model ''natural world'' baseline), and
- a ''2°C world'' (defined using the same method as the 1.5°C world, but for model years within decades when global-average temperatures are between 1.8° and 2.2°C warmer than the corresponding model ''natural world'' baseline).

These definitions follow those used by King et al. (2017) and allow large ensembles of thousands of model years to be generated, particularly for the 1.5° and 2°C worlds, increasing the statistical power of our analysis. This method is similar to the ''time-shift approach'' described by Herger et al. (2015) or ''time-sampling method'' described by James et al. (2017). The majority of the analysis focuses on the change between the 1.5° and 2°C worlds using the natural world as a preindustrial baseline. Sensitivity tests to the choices used in defining these ensembles, such as the use of a late-nineteenth-century reference point as opposed to the natural baseline used here and issues posed by using transient climate simulations, are discussed by King et al. (2017).

Other model variables were used to investigate and assess the causes of climatic changes between 1.5° and 2°C: precipitation, mean sea level pressure (MSLP), 200-hPa zonal winds (U_{200}), 500-hPa geopotential height (Z_{500}), surface downwelling shortwave radiation (RSDS), and 850-hPa specific humidity (Q_{850}). There is a specific focus on the East Asia region for this aspect of the analysis.

Observational datasets were also used for the East Asia component of the study. Gridded surface air temperature from the CRU-TS4.00 dataset (Harris et al. 2014) was extracted to evaluate the CMIP5 model simulations over East Asia and to define a threshold for hot summer temperatures in the region. The equivalent meteorological variables extracted from the CMIP5 ensemble were also analyzed in the ERA-Interim reanalysis (Dee et al. 2011) for comparison of the background synoptic conditions associated with hotter summers in the East Asia region.

Population data prepared by the Global Carbon Project (http://www.cger.nies.go.jp/gcp/population-and-gdp.html) were used to estimate the number of people living in our East Asia region of interest. The data for 2010 were used with the population aggregated over the grid boxes within the East Asia region.

All observational and model data were interpolated to a regular 2° grid. Anomalies in the East Asian temperatures were calculated using a 1961–90 climatology so the observed and model-simulated series could be compared directly. The model temperature anomalies were calculated from corresponding model historical simulations.

b. Scaling definitions

Annual and seasonal temperatures are projected to rise by varying amounts regionally at 1.5° and 2°C of global warming and between these two warming levels (Fig. 1). Stronger warming is projected over the Arctic, especially in boreal winter. There is also greater warming projected over land than oceans and a slight cooling in an area of the North Atlantic to the west of the British Isles. The projected spatial patterns of changes from 1.5° to 2°C of global warming are in line with the temperature changes expected more generally (e.g., Kirtman et al. 2013). The purpose of this study is to examine whether the projected temperature changes scale from warming up to 1.5°C of global warming and to investigate the causes of deviations from this scaling.

First, a scaled local temperature at 2°C global warming was derived simply as a linear extension of the local temperature change from the natural baseline to 1.5°C global warming (Fig. 2a) at each grid box independently of other grid boxes:

$$T_{\text{Scaled\_to\_2}} = T_{1.5} + \frac{T_{1.5(50p)}}{3}.$$

We constructed the scaled distribution by shifting all values in the model-simulated local temperature distribution at 1.5°C, $T_{1.5}$, by one-third of the local median temperature warming in the 1.5°C world, $T_{1.5(50p)}$. The scaled temperatures were calculated using the local median temperature at global warming of 1.5°C, $T_{1.5(50p)}$, in each model separately (to investigate levels of model agreement) and also across the entire ensemble (to estimate the average scaling departures). Scaling departures were estimated by comparing scaled and simulated model temperatures in the 2°C world. Departures D from the scaled temperature are calculated both in degrees Celsius:

$$D = T_{\text{Simulated\_to\_2}} - T_{\text{Scaled\_to\_2}}$$

and as a percentage:

$$D = 100\left(\frac{T_{\text{Simulated\_to\_2}} - T_{1.5}}{T_{\text{Scaled\_to\_2}} - T_{1.5}}\right) - 100.$$

For the idealized example shown in Fig. 2a, $D = +0.67$°C or +100%; that is, the simulated warming is double that expected from scaling.

The scaling applied in this analysis is only to local temperatures and is additive as opposed to multiplicative, such that the scaled 2°C distribution is simply a translation of the 1.5°C distribution. In preserving the shape of the distribution at each grid box there is an assumption that the mean is changing but higher statistical moments are not (Lewis and King 2017), whereas a multiplicative scaling in a warming climate would generally lead to greater variance in the scaled 2°C distribution relative to the 1.5°C distribution. The additive approach also means that going up from 1.5° to 2°C or going down from 2° to 1.5°C produces similar results, as the spatial patterns of scaling departures remain but the sign of the scaling departure is reversed. The scaling departures D are still calculated using $T_{\text{Simulated\_to\_2}}$ in our methodology, which, on average, will have a better estimate of the forced response than $T_{1.5}$.

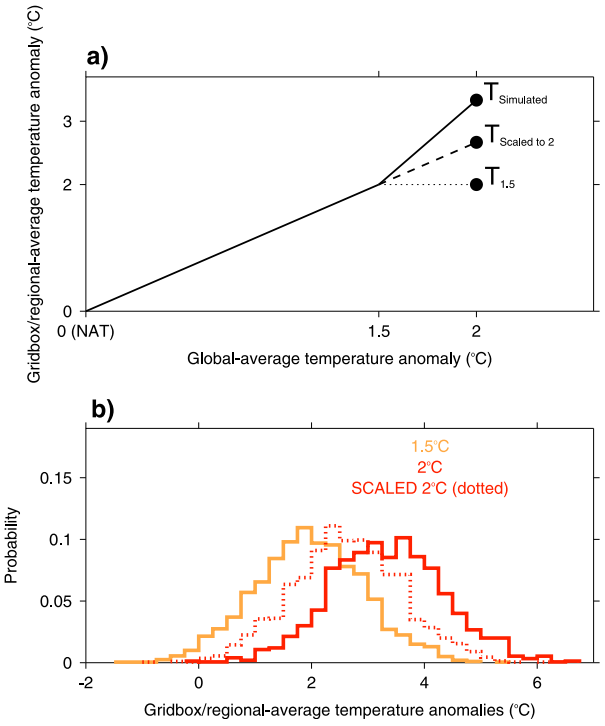

FIG. 2. Schematics illustrating (a) definitions of departures from scaling and (b) the generation of artificial scaled statistical distributions. In the example illustrated here the model median simulated warming is 0.67°C or 100% above the scaled response.

Note that as the scaling is applied to each grid box individually the spatial variance in the scaled 2°C world is increased relative to the 1.5°C world. Our statistical analysis of the scaling departures examines each gridbox temperature distribution independently, such that none of the study relies on the spatial variance in the scaled 2°C world being preserved. In contrast, the statistical analysis of the scaled and simulated 2°C distributions described below require that the scaling not artificially increase the variance or range of the distribution at each grid box.

The representation of the climate at 1.5° and 2°C global warming in each model is a combination of the forced

response and internal variability. The larger the sample size of model years at these warming levels, the better constrained the forced response to anthropogenic forcings. Therefore, we would have greater confidence in model results from individual models with larger ensembles of simulations available, such as CSIRO-Mk3.6.0, compared with models where fewer simulations are used to construct the 1.5° and 2°C worlds, such as ACCESS1.3. In response to this issue, the statistical analysis and model agreement tests discussed below are designed to be insensitive to individual outlier models. A supplementary analysis was also performed comparing the patterns of scaling departures between model years from individual runs of the CanESM2 and CSIRO-Mk3.6.0 models where internal variability differs but the forced response between runs of the same model remains similar.

The use of the trend from a natural baseline to 1.5°C, instead of a smaller global warming increment, reduces the effect of noise in the scaling calculations. The scaling method used here would perform less well in other situations where either the reference warming trend is between smaller global warming increments or the extension global warming increment is larger.

c. *Assessing model agreement and significance of scaling departures*

In addition to estimating the magnitude of the departure from scaling, we also quantified the level of model agreement in the departure from scaling as this provides an indication of the confidence in projected departures. Multiple methods can be used to investigate and quantify model agreement; three of these are compared here.

First, a signal-to-noise ratio was calculated to identify regions for which the multimodel median departure from linear scaling exceeds the standard deviation σ across individual model departures from scaling:

$$S/N = \frac{\overline{D}}{\sigma}.$$

This approach bears some similarity to that used to determine the time of emergence (ToE) in climate variables (e.g., Giorgi and Bi 2009), although the noise is only a measure of intermodel variability in this case, whereas in ToE studies it is often a combination of intermodel variability and internal climate variability. The signal-to-noise ratio provides an indication of the scale to which the multimodel median departure from scaling differs from the variability in scaling departures represented in different models.

Second, we examined the model agreement in the sign of the departure from linear scaling, D. For a particular location, if $D > 0$ for all models or $D < 0$ for all models, then this indicates that there is model consensus (at least among the 16 models used in this analysis) that simulated warming at 2°C is respectively greater or less than that expected from a linear scaling.

Third, we investigated model agreement in the statistical significance of departures from scaling. We estimated whether the statistical distribution of model-simulated temperatures in a 2°C world is significantly different from a scaled distribution from 1.5°C global warming. The scaled and simulated statistical distributions of temperature at 2°C of global warming were compared using a Kolmogorov–Smirnov (KS) test. If the p value associated with the KS test coefficient is less than 0.05 then there is less than a 5% chance that the scaled and simulated temperature distributions at 2°C global warming could be derived from the same sample and, therefore, there is a high likelihood that the scaled and simulated samples are statistically different. This analysis was performed on each CMIP5 model to give a further indication of model agreement in whether local temperature changes in a 2°C world are well projected by a simple scaling from the projected temperature change to 1.5°C of global warming. Note that while the entire ensembles for the 1.5° and 2°C worlds are large, this is not the case for the individual models, so the KS test is not simply detecting significance due to subtle differences between large sample sizes. Also, the use of an additive scaling approach instead of a multiplicative approach reduces the likelihood of ''false positive'' significant results detected using a KS test, by design. The KS test not only detects changes in location, but also in higher statistical moments, so a multiplicative scaling, which would increase spread in the distribution, would result in a greater occurrence of statistically significant differences.

These three metrics for investigating model agreement have different advantages and disadvantages. For example, the KS test between the simulated and scaled distributions is the only test of the three that considers the entire modeled temperature distribution at each grid box, as opposed to the model median. Unlike the other tests, the KS test does not indicate whether a significant result is due to the scaled distribution being warmer or cooler than the simulated distribution.

We are also interested in the potential for larger scaling departures. To assess this possibility, we use the model spread σ, defined previously, and plot scaling departures for the multimodel median $\pm\sigma$. Other methods could be used to investigate more extreme possible scaling departures, but by using the model spread, as opposed to plotting the most extreme departures across the ensemble, this method is less sensitive to individual model outliers. Note that any measure

TABLE 1. CMIP5 models and simulations used in this study. In bold are model simulations used for calculating natural baseline and the 1.5° and 2°C warmer worlds. Other historical simulations were only used for model evaluation. All models apart from GFDL-CM3 (italicized) were used in East Asian event attribution analysis. GFDL-CM3 did not pass the model evaluation test for use in this component of the study. (Expansions of acronyms are available online at http://www.ametsoc.org/PubsAcronymList.)

Model	Historical	HistoricalNat	RCP2.6	RCP4.5	RCP6.0	RCP8.5
Time period	(1861–2005)	(1901–2005)	(2006–2100)			
ACCESS1.3	**1**, 2, 3	**1**		**1**		**1**
BCC-CSM1.1	**1**, 2, 3	**1**	**1**	**1**	**1**	**1**
CanESM2	**1**, **2**, **3**, **4**, **5**	**1, 2, 3, 4, 5**	**1**, **2**, **3**, **4**, **5**	**1**, **2**, **3**, **4**, **5**		**1**, **2**, **3**, **4**, **5**
CCSM4	**1**, **2**, 3, **4**, 5, **6**	**1, 2, 4, 6**	**1**, **2**, **4**, **6**	**1**, **2**, **4**, **6**	**1**, **2**, **4**, **6**	**1**, **2**, **4**, **6**
CESM1-CAM5	**1**, **2**, **3**	**1, 2, 3**	**1**, **2**, **3**	**1**, **2**, **3**	**1**, **2**, **3**	**1**, **2**, **3**
CNRM-CM5	**1**, **2**, 3, **4**, 5, 6, 7, 8, 9, 10	**1, 2, 4**	**1**	**1**		**1**, **2**, **4**
CSIRO-Mk3.6.0	**1**, **2**, **3**, **4**, **5**, 6, 7, 8, 9, 10	**1, 2, 3, 4, 5**	**1**, **2**, **3**, **4**, **5**	**1**, **2**, **3**, **4**, **5**	**1**, **2**, **3**, **4**, **5**	**1**, **2**, **3**, **4**, **5**
GFDL-CM3	**1**, 2, 3, 4, 5	**1**	**1**	**1**	**1**	**1**
GISS-E2-H	**1**, **2**, 3, 4, 5	**1, 2**	**1**	**1**, **2**	**1**	**1**, **2**
GISS-E2-R	**1**, **2**, 3	**1, 2**	**1**	**1**, **2**	**1**	**1**, **2**
HadGEM2-ES	**1**, **2**, **3**, **4**, 5	**1, 2, 3, 4**	**1**, **2**, **3**, **4**	**1**, **2**, **3**, **4**	**2**, **3**, **4**	**1**, **2**, **3**, **4**
IPSL-CM5A-LR	**1**, **2**, **3**, 4, 5, 6	**1, 2, 3**	**1**, **2**, **3**	**1**, **2**, **3**	**1**	**1**, **2**, **3**
IPSL-CM5A-MR	**1**, 2, 3	**1**	**1**	**1**	**1**	**1**
MIROC-ESM	**1**, 2, 3	**1**	**1**	**1**	**1**	**1**
MRI-CGCM3	**1**, 2, 3	**1**	**1**	**1**	**1**	**1**
NorESM1-M	**1**, 2, 3	**1**	**1**	**1**	**1**	**1**

of spread across models includes internal variability in single realizations. On local scales particularly, this variability likely contributes to nonlinearities in the forced response (Hawkins and Sutton 2009) but, as mentioned previously, some processes such as sea ice changes may also contribute to nonlinearities.

Also, we do not specifically define what constitutes a ''large'' or ''small'' scaling departure but instead present departures in both absolute and percentage terms for the multimodel average and possible larger scaling departures to allow readers to make their own interpretations. Impacts of nonlinear warming patterns would likely differ between locations and seasons, so a single definition would not be helpful.

Additional sensitivity tests were performed to test the robustness of this study. These tests are described in more detail in the online supplemental material.

d. *Understanding the causes of scaling deviations*

After identifying regions where scaling from 1.5° to 2°C provides a poor representation of temperature projections in a 2°C world, an analysis of the causes for nonlinearities in regional warming to a 2°C world was undertaken. Changes in atmospheric circulation patterns and thermodynamic variables were calculated to examine possible mechanisms behind departures from scaling. Variables including 200-hPa zonal winds, 500-hPa geopotential height, mean sea level pressure, surface downward shortwave radiation, and 850-hPa specific humidity were composited for the 1.5° and 2°C worlds and changes analyzed. These changes were calculated across the CMIP5 ensemble and in individual models. East Asia was identified as a region of interest and studied in greater detail due to a large nonlinearity in warming over the area and a high population exposure to climatic changes.

e. *Understanding the influence of scaling deviations on extremes*

To highlight the importance of nonlinear regional warming we examined whether there was an effect on the likelihood of extremes. Using the example of the East Asia region in boreal summer (JJA) the likelihoods of extreme heat in a natural world, the current world, a 1.5°C world, a simulated 2°C world, and a scaled 2°C world were compared. The method used for this component of the analysis follows from event attribution studies that quantify the role of anthropogenic influences in the likelihood of an extreme occurring (e.g., Lewis and Karoly 2013; King et al. 2015b).

First, the model-simulated East Asia summer temperature anomalies over the historical period of 1951–2005 were compared with the observed (CRU-TS4.0) summer temperature anomaly series over this time. Anomalies in both the observed and modeled time series were calculated from a 1961–90 climatology. Any models with at least one-third of historical simulations being significantly different ($p < 0.05$) from the observational series, as measured by a KS test, were removed from analysis (marked in Table 1). The ability of the CMIP5 ensemble to capture the trend in East Asian summer temperatures was also examined over the common 1970–2016 and 1990–2016 periods.

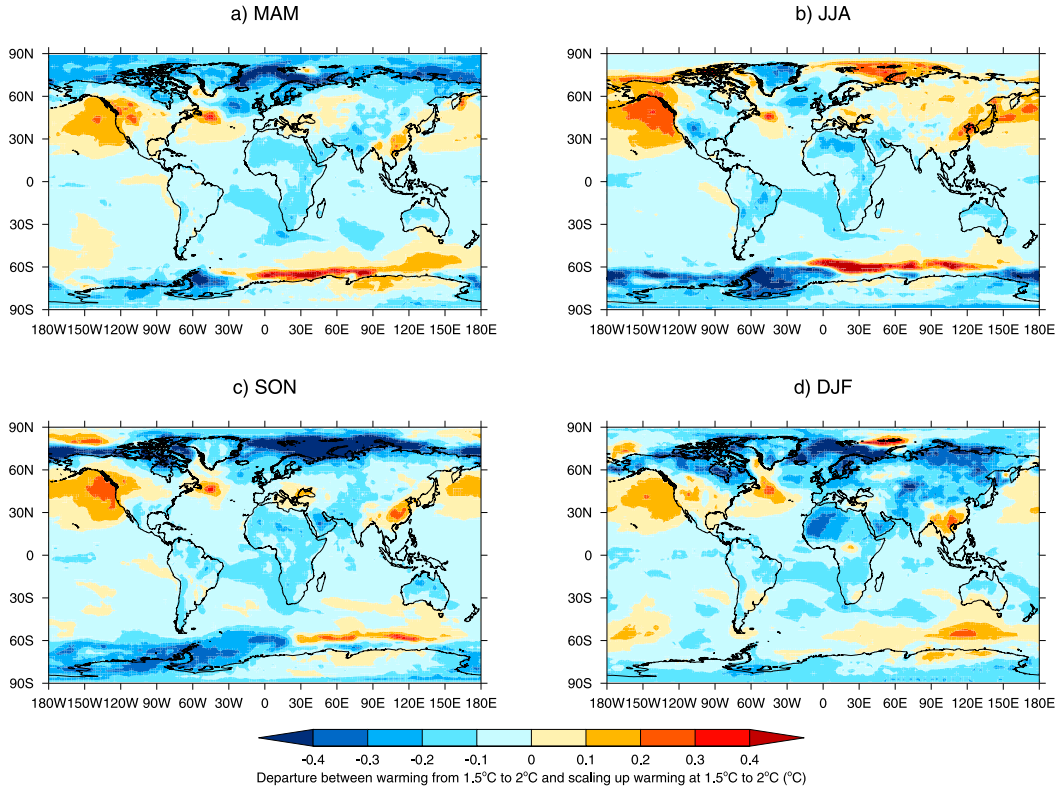

FIG. 3. Maps of the departure from linear scaling in the model ensemble median seasonal temperature from 1.5° to 2°C of global warming in units of degrees Celsius for (a) MAM, (b) JJA, (c) SON, and (d) DJF.

An event attribution framework was used to investigate whether there was a significant change in the likelihood of extreme heat between the five scenarios using the remaining CMIP5 models that passed the evaluation test. The probability of exceeding the threshold of the existing record hot summer in the region (+1.25°C anomaly in 1994) was computed in each scenario. To ascertain the sampling uncertainty on these probabilities, the complete model simulations within each scenario were 50% bootstrap resampled 10 000 times. The probabilities of extreme heat were recalculated and 90% confidence intervals were extracted. The risk ratio (RR) of extreme heat in the simulated 2°C world relative to the scaled 2°C world was simply calculated as

$$\mathrm{RR} = \frac{P_{\mathrm{Simulated}}}{P_{\mathrm{Scaled\_to\_2}}},$$

where $P_{\mathrm{Simulated}}$ is the probability of extreme summer temperatures (exceeding the +1.25°C threshold) in the modeled 2°C world, and $P_{\mathrm{Scaled\_to\_2}}$ is the probability of extreme heat in the scaled 2°C scenario. The risk ratio was also calculated using the pairs of 10 000 bootstrapped subsamples and a conservative 10th percentile estimate was extracted.

3. Results

a. Global analysis

For much of the globe, our multimodel analysis suggests that scaling up the warming from a natural baseline to 1.5°C onward to a 2°C world might provide a reasonable approximation of the changes that could be expected. Over most regions, the departure from a scaled response in the average temperature is less than 0.2°C, with larger departures in parts of the high latitudes (Fig. 3). There is also a slight seasonal dependence with simulated warming exceeding a simple scaling in the summer hemisphere more than during winter and this is especially clear over Eurasia (Figs. 3b,d). Some regions show simulated warming that is consistently above a scaled response throughout the year, including the North Pacific, an area of the northwest Atlantic, and eastern China.

The signal-to-noise ratio in the modeled departures from scaling (Fig. 4) highlights equatorial regions where both the signal and the noise (i.e., the spread across the model ensemble) are relatively small when compared with higher latitudes where the signal is higher but the uncertainty in the signal is greater. In the tropics there is a tendency for below-scaled warming projected at 2°C,

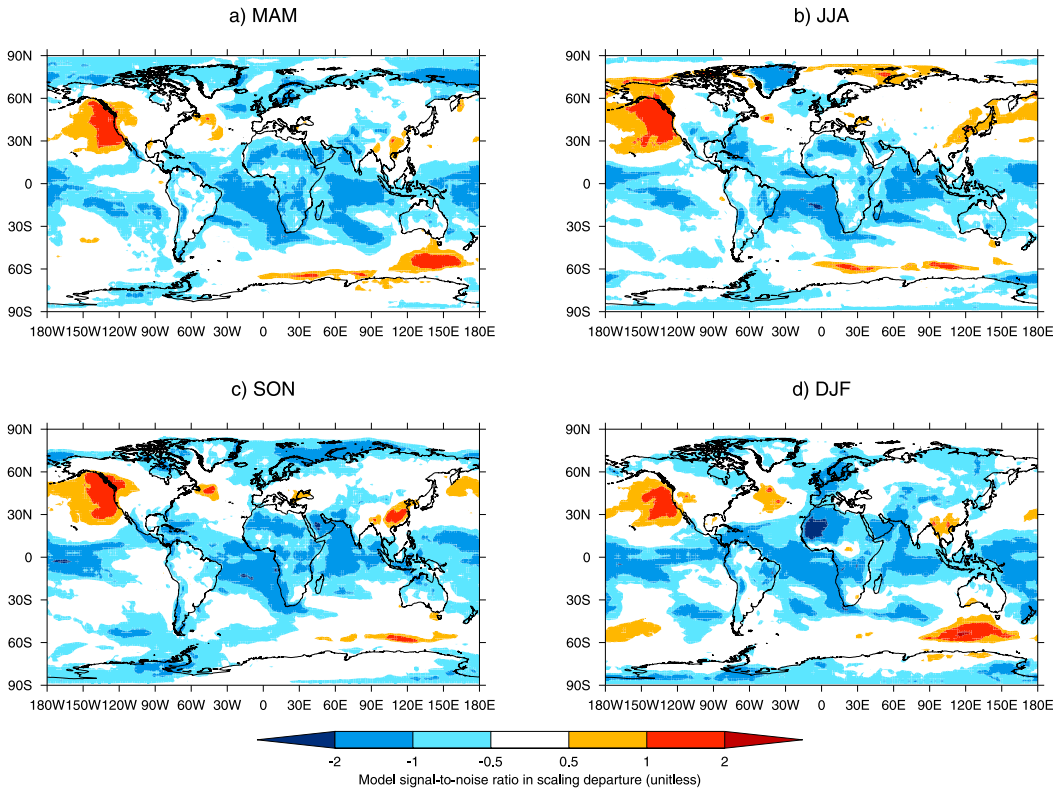

FIG. 4. The signal-to-noise ratio in the departure from a linear scaling from 1.5° to 2°C where signal is defined as the multimodel median departure (as shown in Fig. 3) and the noise is the standard deviation across the distribution of each model's average departure from scaling. Signal-to-noise ratios of less than 0.5 in magnitude are not shown.

and this is also seen over northwestern Africa in boreal winter. In contrast, the northeast Pacific region is again highlighted as a region where above-scaled warming is projected.

We find that considerable model spread in scaling departures results in potential large deviations from scaling projected in some models (Fig. 5). At high latitudes there is the possibility of as much as 0.5°–1°C of a scaling departure in either an acceleration or deceleration of local warming. These are large potential changes in the rate of overall warming even for those locations. An estimation of the contributions of internal variability and nonlinearities in the forced response would require large initial conditions ensembles.

When we investigate the level of model agreement on the sign of the deviation from scaling in the model median temperature in a 2°C world, we find that over the North Pacific and eastern China there is greater consensus that simulated warming exceeds scaling (Figs. 6a,b). In many equatorial and subtropical areas there is agreement that the level of warming is likely to be below a scaled response. Over the North Atlantic there are low levels of model agreement. This is related to the CMIP5 models simulating areas of freshening and cooling (Zhang and Wang 2013) in slightly different locations (e.g., Menary and Wood 2018) and the different model representations of the mean state and change in sea ice cover and the Atlantic meridional overturning circulation (Collins et al. 2013; Tebaldi and Arblaster 2014). Comparing entire distributions of seasonally averaged temperatures between the simulated and scaled 2°C worlds, as measured by a KS test and using a p level of 0.05, most models show statistically significant differences over most locations (Figs. 6c,d). However, there is a lack of a clear geographical pattern in the areas where models agree that scaling and simulated temperature distributions are significantly different from each other. There is an indication that over the tropical east Pacific the CMIP5 models have greater similarity in the scaled and simulated 2°C worlds.

Departures from scaling can be represented in different ways. By showing departures from scaling only in degrees Celsius (as in Fig. 3) we are more likely to see greater departures where the overall warming trend is greater, so we also show percentage departures from scaling (Fig. 7). Over the North Atlantic there are larger percentage departures from scaling, which is unsurprising given the weak temperature trends in that region (Fig. 1).

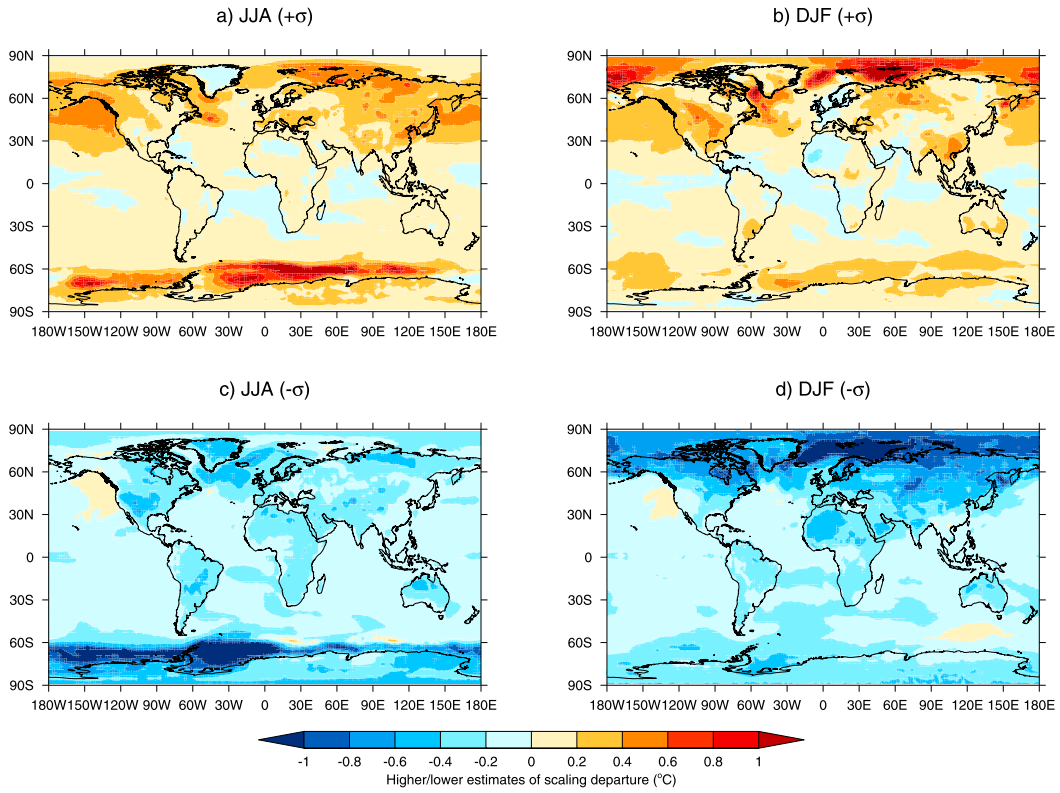

FIG. 5. As in Fig. 3, but showing possible higher or lower estimates of the scaling departure (resulting from both nonlinear forced responses in single models as well as unforced internal variability) calculated as the median plus or minus the standard deviation across scaling departures at each grid box. (a),(b) Possible above-average scaling departures for JJA and DJF, respectively. (c),(d) Possible below-average scaling departures for JJA and DJF, respectively.

Over large areas of the southern Atlantic and Indian Oceans the multimodel-average warming from the 1.5° to 2°C scenario is around 20% less than would be expected from a simple scaling and there is strong model agreement in both the sign and the significance of this departure from scaling. In contrast, in eastern China the simulated 2°C world is at least 20% warmer than would be expected from a simple scaling up from 1.5°C and there is strong model agreement here on both the sign and significance of the departure from scaling.

Projected precipitation changes from 1.5° to 2°C largely follow the ''wet get wetter, dry get drier'' paradigm (Fig. 8; Held and Soden 2006). There is a tendency for drying of the subtropics (e.g., northern Africa, the Mediterranean, southern Africa, and western Australia) and increasing seasonal-scale precipitation in other regions. There is model agreement in the sign and the significance of increases in seasonal precipitation totals over the northern high latitudes, especially in boreal winter. These are areas where there is already an indication of an attributable signal in the increasing precipitation to human-induced climate change (e.g., Min et al. 2011; King et al. 2015a). There is also model agreement for an increasing precipitation signal over the tropical Pacific and some indication of agreement on a drying trend in areas of Brazil.

Changes in atmospheric circulation, as indicated using mean sea level pressure (MSLP), are greatest in the high latitudes (Fig. 9). While the average changes in MSLP are not substantial (typically below 0.5 hPa) these are seasonal-average values of MSLP in large model ensembles so we would not expect to see very large changes.

There are few areas outside the tropics where there is model agreement on the sign and significance of the change in MSLP from the 1.5° to 2°C worlds. This is unsurprising given that internal variability dominates intermodel spread in extratropical MSLP projections (Deser et al. 2012). Gillett and Stott (2009) found that the high internal variability in MSLP outside the tropics resulted in detectable anthropogenic influences only in low-latitude regions. However, there are slight tendencies toward increased MSLP to the west of Europe and reduced MSLP to the north in both boreal autumn and winter. In austral autumn and winter there is also an

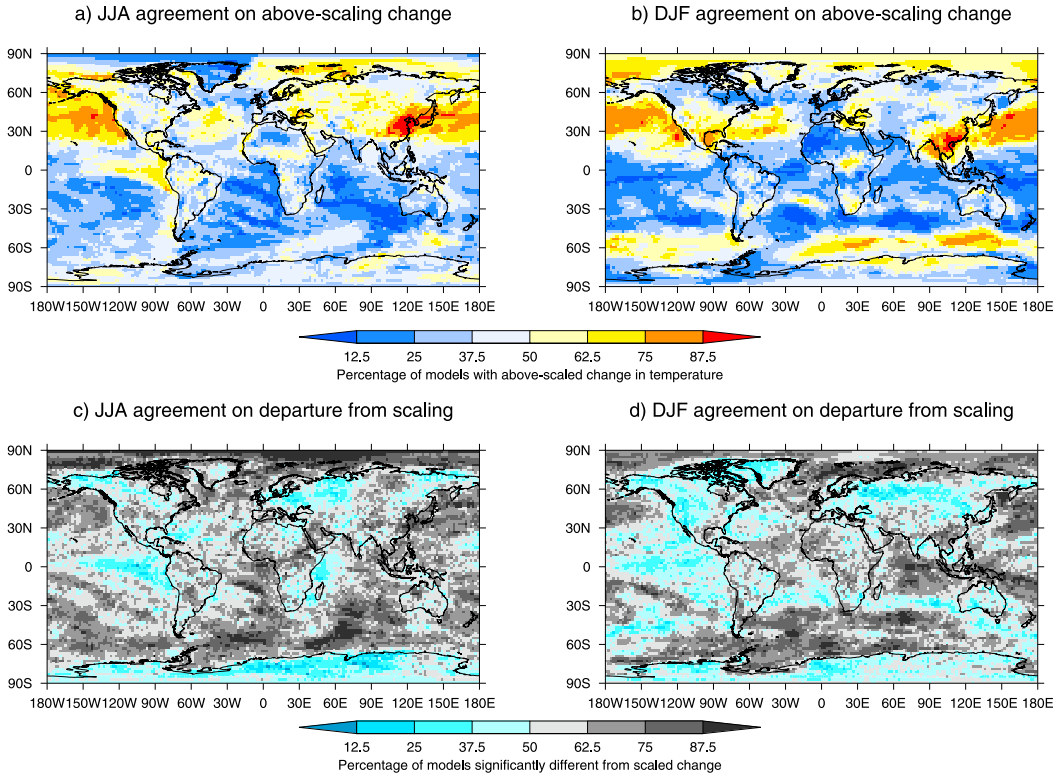

FIG. 6. Maps indicating the levels of model agreement in deviations from linear scaling. (a),(b) Proportion of models where the sign of deviation in the simulated median temperature at 2°C of global warming from scaling of the median temperature from 1.5° to 2°C global warming is positive, and (c),(d) proportion of models in which the simulated seasonal-average temperature distribution at 2°C of global warming is significantly different ($p < 0.05$) from the scaled distribution at 2°C global warming for JJA and DJF temperatures, respectively.

indication of a poleward movement in the Southern Hemisphere extratropical storm track (e.g., Arblaster and Meehl 2006) with a similar multimodel change in austral spring and summer likely obscured by ozone recovery, which has an opposing effect to greenhouse gases (Eyring et al. 2013). Zonal-mean analysis of the changes in MSLP from 1.5° to 2°C in the climate models highlights the different latitudes at which the MSLP is decreasing the most, even after zonal averaging, between models (Fig. 10). It was hypothesized that a relationship between model-simulated zonal-mean temperature scaling departures and zonal-mean MSLP might be found, especially in high-latitude areas where there are large simulated changes in the storm track. No clear links could be drawn between simulated MSLP and scaling departures across the different CMIP5 models in the zonal-mean analysis. However, the zonal-mean analysis again illustrates the possibility of large nonlinear local warming between the Paris Agreement targets, especially at high latitudes.

It is difficult to understand scaling departures in temperature through global-scale study or zonal-mean analysis. Regional studies will likely yield clearer results on mechanisms behind nonlinear local warming from 1.5° to 2°C global warming. We focus on East Asia due to its large consistent scaling departures and high population exposure to climate changes. Note that other regions also show high model agreement in scaling departures such as northwest Africa in boreal winter. For the sake of brevity we only examine the East Asia region here.

b. East Asia regional analysis

A comprehensive analysis of the above-scaling regional warming over East Asia (110°–130°E, 30°–45°N; Fig. 11a) projected at 2°C of global warming was conducted. The analysis was for boreal summer (June–August) only. A reason for selecting this region is that it includes many major cities, such as Beijing and Shanghai in China and Seoul in South Korea. The overall population of the East Asia region, following our definition, was 722 million in 2010 using the Global Carbon Project dataset (i.e., more than one-tenth of the global population at the time). It is known that climate change has

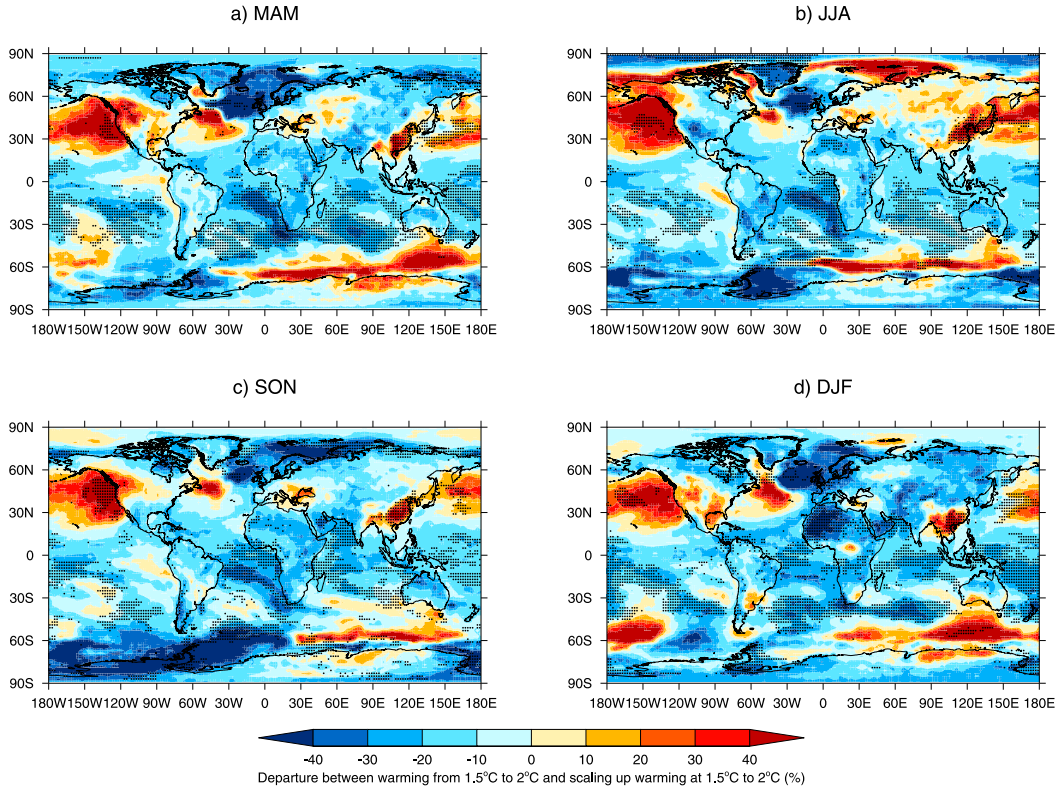

FIG. 7. Maps of the percentage departure from linear scaling in seasonal temperature from 1.5° to 2°C of global warming. Stippling indicates where there is at least 75% model agreement on the sign of deviation from scaling and greater than half the model-scaled 2°C distributions are significantly different from the corresponding model-simulated 2°C distributions.

increased the numbers of casualties in recent European heatwaves (Mitchell et al. 2016a); while no comparative analysis exists for East Asia, climate change is already contributing to heatwaves (Ma et al. 2017; Sun et al. 2014, 2017) and their impacts in the region. The impacts of greater summertime warming in this region could therefore be very large, so understanding why the CMIP5 ensemble projects above-scaling warming over East Asia is important.

The major factor is a reduction in aerosol concentrations in the 2°C ensemble relative to the 1.5°C ensemble. The anthropogenic aerosol emissions of the late twentieth and early twenty-first centuries over East Asia have had a cooling effect on summer temperatures, cushioning some of the warming in the region otherwise expected. In the climate projections for the twenty-first century, these aerosol concentrations in the atmosphere decrease, under the assumption that action is taken to reduce their emission, accelerating warming in the coming decades (Xu et al. 2018). There are higher concentrations of anthropogenic aerosols, such as black carbon and sulfates (Lamarque et al. 2011), in the early twenty-first century (when the 1.5°C ensemble is predominantly composed) compared to the mid to late twenty-first century (when more years contribute to the 2°C ensemble; King et al. 2017).

The evidence for the aerosol effect can be seen in the change in downwelling shortwave radiation (RSDS) at the surface (Fig. 11b). In the 2°C world there is 2%–4% higher RSDS compared to the 1.5°C world on average. The pattern of increased shortwave radiation also matches strongly with the area of above-scaling warming at 2°C (the pattern correlation for the entire area shown in Figs. 11a and 11b is 0.64).

Another illustration of the aerosol influence on the departure from scaling is seen in the stronger model agreement on the sign and significance of above-scaling warming when using only the RCP4.5 (moderate emissions) scenario relative to only using the RCP8.5 (high emissions) scenario (Figs. 7a,c). As the 1.5° and 2°C worlds are farther apart in timing under RCP4.5 [see the supplemental information of King et al. (2017)] and the decline in aerosol emissions between RCP4.5 and RCP8.5 is similar, the difference in the aerosol influence is also larger.

Other changes exist between the 1.5° and 2°C worlds over East Asia. These include increases in 500-hPa

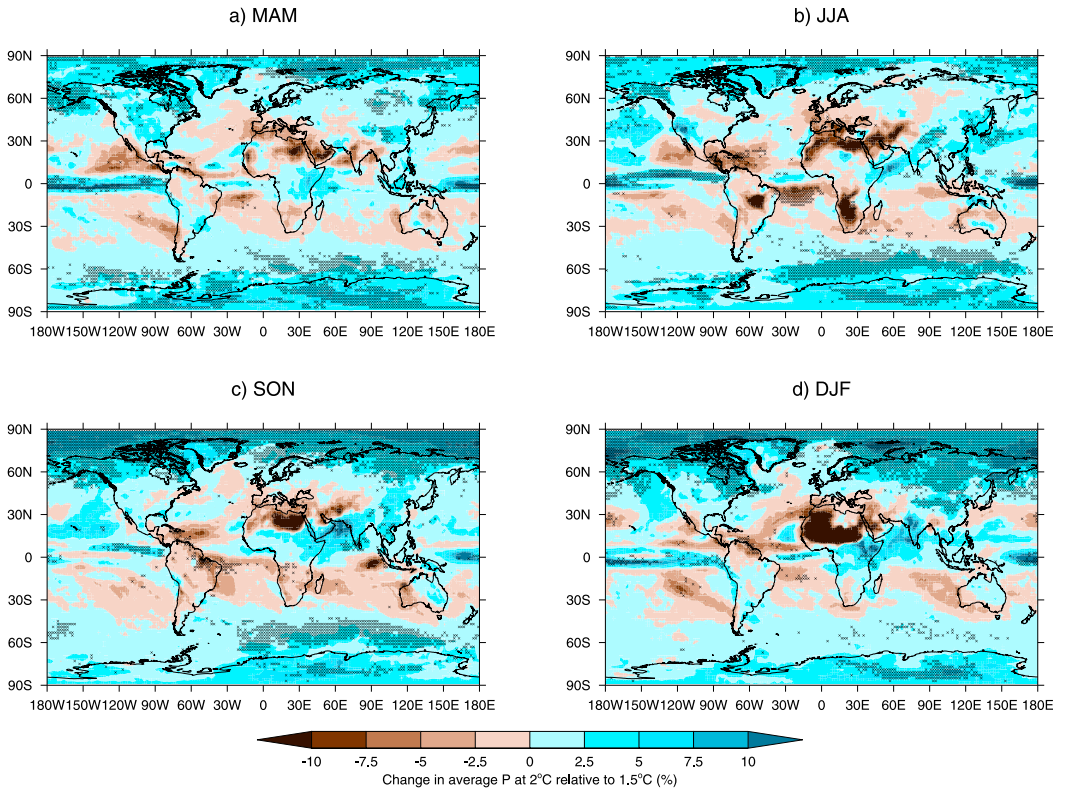

FIG. 8. Maps of the median change in precipitation from 1.5° to 2°C of global warming. Hatching indicates where there is at least 75% model agreement on the sign of precipitation change and greater than half the model-simulated 2°C distributions are significantly different than the corresponding model-simulated 2°C distributions.

geopotential height (Fig. 11c) and 850-hPa specific humidity (Fig. 11d), although these are both common to much of the world. There is also a decrease in mean sea level pressure over the East Asia domain and to the north and east (Fig. 11e) and a decrease in upper-level zonal winds to the south of the region with a slight increase to the north (Fig. 11f), albeit with low significance in the change.

Some of these synoptic-scale summer-averaged changes are similar to the characteristics associated with shorter-scale heatwaves in eastern China (e.g., Freychet et al. 2017). Freychet et al. (2017) found that heatwaves in this region are dynamically forced and initiated with increased geopotential height and surface solar radiation. They also identified a reduced MSLP anomaly to the northeast of the region during heatwaves, which they speculated was due to the formation of a meridional circulation, a dynamical response to the local heating. There are limitations in making parallels between atmospheric conditions associated with heatwaves and hotter summers, of course, but many of the identified ingredients that are associated with heatwaves in East Asia are projected to become more intense, on average, in a 2°C world relative to a 1.5°C world. Within individual CMIP5 models, hotter summers in the 1.5° and 2°C warmer worlds are associated with many of these atmospheric anomalies as is the case in the ERA-Interim reanalysis (Table 2).

We explore the simulated changes in these variables further by comparing the responses to 2°C global warming in the 16 CMIP5 models used here separately. First, we identify a range in the warming from 1.5° to 2°C relative to the warming up to 1.5°C across the models (Fig. 12a). All the models show greater warming to 2°C than expected from scaling, but some are only just above the scaled response from 1.5°C (e.g., ACCESS1.3 and CNRM-CM5) whereas other models warm far more than scaling would predict (e.g., GISS-E2-H and MIROC-ESM). The models that have the largest increase in summer-average 500-hPa geopotential height over East Asia between 1.5° and 2°C also tend to have the greatest warming from 1.5° to 2°C (Fig. 12b) and the greatest exceedance of a scaled response (not shown). In addition, the models with the greatest increase in 850-hPa specific humidity and the largest decreases in MSLP to the northeast of the region also tend to be the models with the greatest warming to 2°C global warming (Figs. 12c,d).

While the initiation of an above-scaling warming in East Asia is due to the reduction in anthropogenic

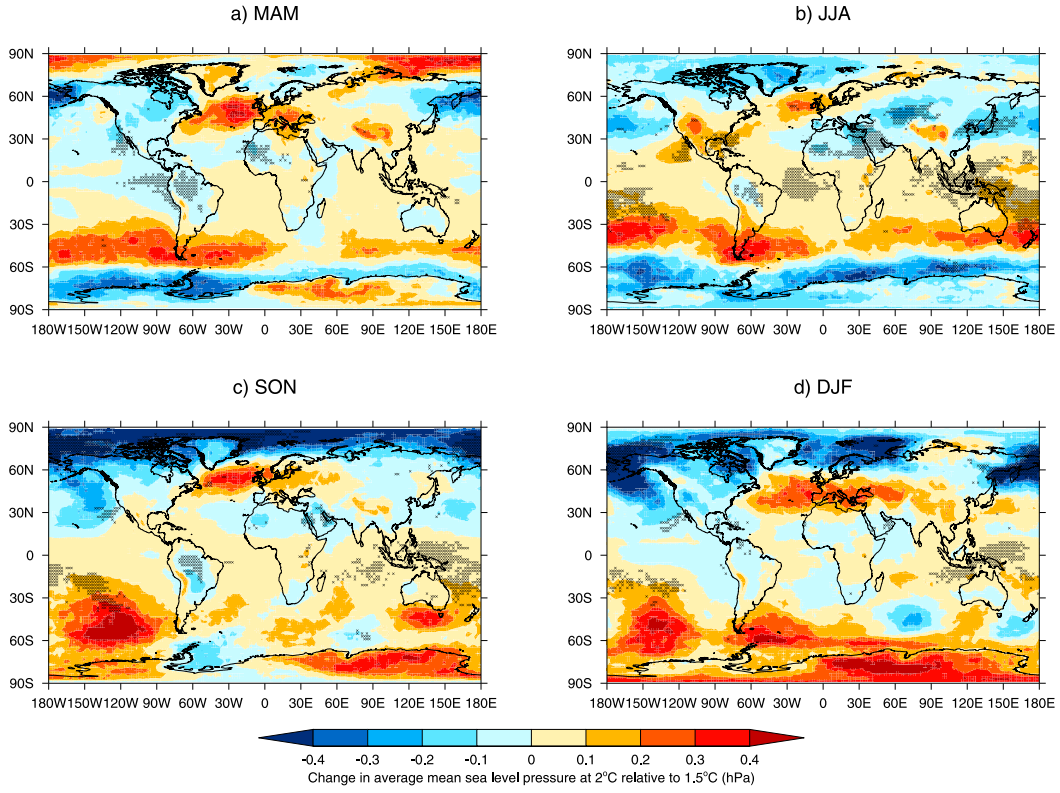

FIG. 9. As in Fig. 8, but for mean sea level pressure.

aerosol emissions through the CMIP5 projections, the increased solar radiation and thickness of the lower to middle atmosphere over the region also have associated dynamical changes, as seen in the MSLP reduction to the northeast. The models with the greatest simulated exceedance of a scaled warming to 2°C tend to have the strongest changes in these variables.

The consequences of East Asian summer simulated warming at 2°C exceeding a scaled warming are investigated by quantifying the change in record hot summer-average temperatures in the region. The current record hot summer for the region was in 1994, although other recent summers in the observational series have been almost as hot. The summer of 1994 was 1.25°C hotter than the 1961–90 climatology (based on CRUTS4.0.0). We compare the likelihood of hot summers exceeding the observed record between the natural, current, 1.5°C, simulated 2°C, and scaled 2°C worlds.

There is a warming trend in both observed and simulated East Asian summer temperatures over recent decades (Figs. 13a–c). Using CMIP5 we find a shift in the model-simulated summer temperature anomalies in the East Asia region with a warming from the natural-world to current-world scenarios (Fig. 13d). The 1.5°C and simulated 2°C scenarios are warmer still, but the scaled 2°C scenario is slightly cooler than the simulated 2°C world. The frequency of summers hotter than the observed record anomaly was compared between the five scenarios (Fig. 13e). In a natural world the chance of a hot summer exceeding the 1994 record is very low (best estimate of 3%). Under current world conditions (2006–26) the chance of seeing a new hot summer record is estimated at around 1 in 3 for any given year. The fact that we have not seen a recent heat record, despite being more than halfway through the current world period, could be due to a number of reasons including model bias in the hot tail of the distribution, natural decadal variability reducing the likelihood of a new heat record in the observed series, or simply chance. Given that the models perform well in capturing the summer temperature variability and trends in recent decades (Figs. 13b,c) it is unlikely, but possible, that there is a model deficiency.

In the 1.5°C world, a hot summer exceeding the 1994 record is likely to occur in around one in every two years whereas in a 2°C world the frequency increases to at least three-quarters of years (best estimate 83% of years). If, however, we scale East Asia summer temperatures up to 2°C as an extension from the warming from the natural baseline to 1.5°C we find a reduced

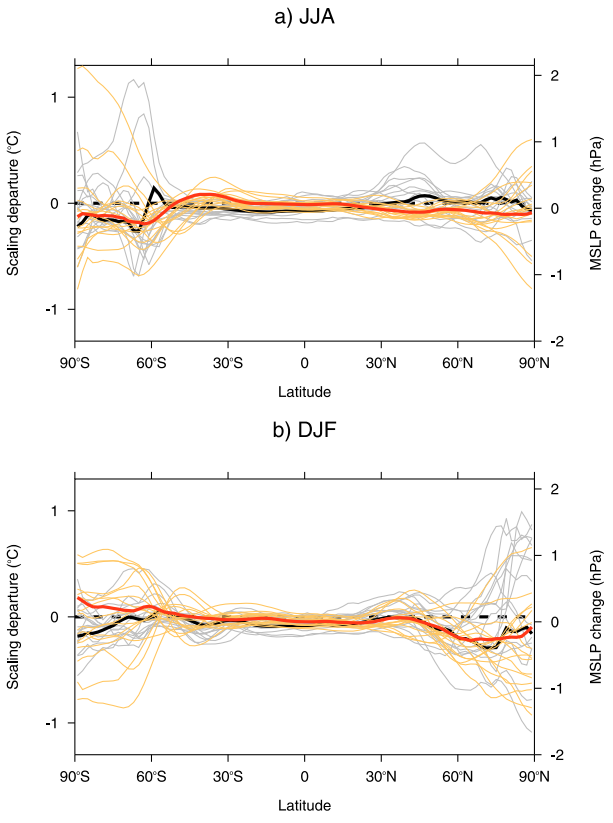

FIG. 10. Zonal-mean analysis of (a) JJA and (b) DJF scaling departures D for seasonal temperatures per model simulation (gray) and for the model-ensemble median (black), showing zonal-mean changes of average MSLP at 2°C minus 1.5°C per model simulation (orange) and for the model-ensemble median (red).

frequency of extreme hot summers (best estimate 77%) relative to the simulated 2°C world. Comparing the scaled and simulated 2°C worlds and employing a risk ratio methodology on the bootstrapped subensembles (described in section 2), we find that it is *very likely* (greater than 90% confidence) that there is an increased probability of record hot summers in East Asia in the simulated 2°C world relative to the scaled 2°C world.

4. Discussion and conclusions

Scaling of local and regional temperatures due to global warming can be conducted in different ways (e.g., Good et al. 2015; Seneviratne et al. 2016). Our method uses the lower Paris Agreement global warming target of 1.5°C and assesses whether the local temperature response to global warming at that level can act as a guide as to the temperature response at the higher Paris Agreement target of 2°C global warming through a linear extension of the warming to 1.5°C. This is an important area of study as an incorrect assumption of a linear response of local temperature to global warming could leave people and ecosystems ill prepared for higher levels of global warming, especially for extreme heat events.

We note that the question of nonlinear change can be framed in two different ways: Will the change from a 1.5°C world to a 2°C world be nonlinear, or is the underlying forced signal nonlinear? It is more straightforward to address the first question given our model simulations, but we have taken steps to attempt to answer the second question through our methodology and sensitivity testing.

In this study we utilize the CMIP5 ensemble of model projections. Our analysis is based on both the model ensemble (which has a large sample of model years at the 1.5° and 2°C global warming levels) and on individual models (which allows for assessment of model agreement and different model responses). By combining these approaches, we provide a thorough and comprehensive analysis on the linearity of warming from 1.5° to 2°C of global warming.

For large parts of the world we find that the multimodel response to scaling up projected warming at the 1.5°C level to the 2°C level provides a reasonable approximation of the warming simulated at 2°C, but that individual model results illustrate the potential for nonlinear local warming due to variability or nonlinearities in the forced response in one model. Across most of the world, the ensemble of models as a whole does not show a consistent or significant departure from scaling up warming from 1.5° to 2°C. For such regions it is possible that local warming up to the global 1.5°C level may provide a good guide for the temperatures that could be expected at 2°C of global warming. We note that in some cases, however, this may be due to internal variability and model spread preventing detection of a departure from linear scaling. Individual models show larger deviations, so for a single realization, such as the real world, we cannot exclude the possibility of large scaling departures.

We examine different metrics for measuring statistical significance and model agreement in departures from linear temperature scaling, so as to provide a comprehensive assessment. In general, there is a lack of sensitivity to the statistical test that is used to determine where prominent departures from scaling exist. After considering different approaches, we combined two of the tests and use stippling to indicate regions where there is both at least 75% model agreement on the sign of deviation from scaling and greater than half the model-scaled 2°C distributions are significantly different ($p < 0.05$ using a KS test) from the corresponding model-simulated 2°C distributions. No single test perfectly captures both the significance and agreement of

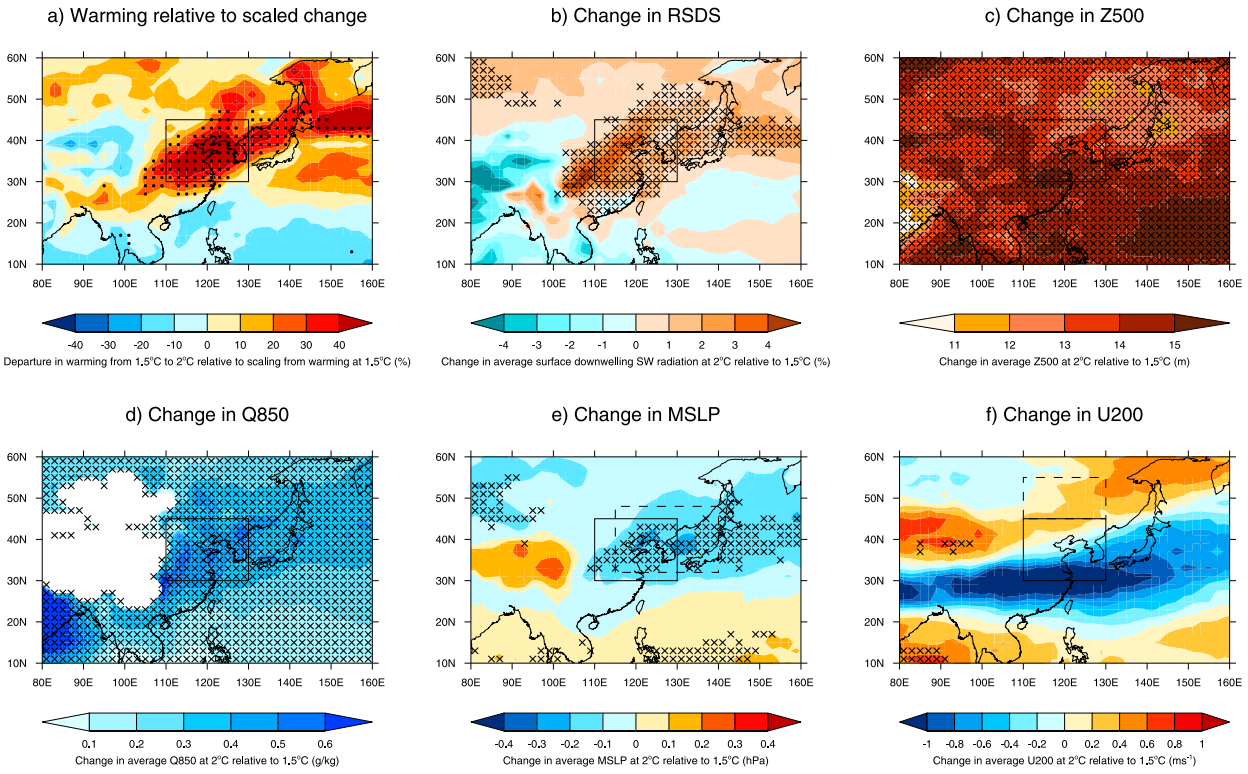

FIG. 11. (a) Map showing the departure in simulated JJA surface air temperature change from a scaled 1.5° to 2°C warming over the East Asia region. Stippling in (a) indicates where there is at least 75% model agreement on the sign of deviation from scaling and more than half the model-scaled 2°C distributions are significantly different than the corresponding model-simulated 2°C distributions. Also shown are maps of simulated changes in JJA (b) surface shortwave downwelling radiation, (c) 500-hPa geopotential height, (d) 850-hPa specific humidity over East Asia, (e) mean sea level pressure, and (f) 200-hPa zonal wind. In (b)–(f) hatching indicates where there is at least 75% model agreement on the sign of change and greater than half the model-simulated 2°C distributions are significantly different than the corresponding model-simulated 1.5°C distributions. The box shows the region of interest and the dashed line boxes show where different regions of study were used for specific variables. The boxes to the north and northeast for zonal winds aloft and MSLP respectively are similar to those of Freychet et al. (2017).

model departures from scaling, so a combination of tests was most useful. The thresholds used in these tests do not require model consensus, which makes them less sensitive to outliers where internal variability is more likely to play a greater role.

We do not find a large dependence in scaling departures on the RCP scenario used with broadly similar patterns of departures from scaling simulated using RCP4.5 and RCP8.5. The results based on RCP2.6 alone (the scenario that is closest to stabilization) are also broadly similar and the precipitation change based solely on RCP2.6 is similar to that for the entire ensemble (Fig. 8; see also Fig. S4 in the online supplemental material). The similarity in temperature scaling departures and precipitation changes comes despite the different combinations of forcings used under each of these scenarios. The likely reason for this is that for relatively low levels of global warming, such as the Paris Agreement levels, the combination of forcings under each RCP is less different than it would be at higher global warming levels. At relatively low levels of global warming the temporal differences in forcing combinations play a greater role than the choice of RCP scenario used. There are substantial differences in other forcings, such as land-use cover of different vegetation types, between the RCP scenarios over the twenty-first century (van Vuuren et al. 2011; Hurtt et al. 2011). Again, the divergence is also largest later in the projections, resulting in a relatively weak influence for low levels of global warming like the Paris targets.

The model responses to the RCP scenarios lead to climates that pass through the 1.5°C level and, in most cases, the 2°C global warming level. The models are not in equilibrium at the Paris Agreement global warming levels, so our results are of more relevance to the climates at the target levels likely to be experienced over the next century assuming there is no rapid reduction in greenhouse gas emissions in the next few years.

TABLE 2. Correlation coefficients (Spearman's rank) between JJA temperatures in the East Asia region and the meteorological variables analyzed in both ERA-Interim (1979–2016) and CMIP5 models in the 1.5° and 2°C worlds. In bold are correlation coefficients that are statistically significant at the 5% level.

	U200		Z500		MSLP		RSDS		Q850	
	0.59		**0.77**		**−0.36**		**0.50**		**0.53**	
ERA-Interim	1.5°C	2°C	1.5°C	2°C	1.5°C	2°C	1.5°C	2°C	1.5°C	2°C
ACCESS1.3	**0.38**	**0.62**	**0.70**	**0.71**	**-0.53**	−0.19	**0.57**	**0.7**	0.27	0.22
BCC-CSM1.1	**0.36**	**0.35**	**0.60**	**0.49**	−0.04	**−0.37**	**0.48**	**0.66**	**0.24**	0.09
CanESM2	**0.17**	**0.11**	**0.47**	**0.50**	**−0.44**	**−0.50**	**0.56**	**0.62**	0.05	**0.12**
CCSM4	**0.46**	**0.43**	**0.56**	**0.55**	**−0.16**	**−0.26**	**0.52**	**0.52**	**0.37**	**0.36**
CESM1-CAM5	**0.48**	**0.42**	**0.77**	**0.70**	**−0.22**	**−0.24**	**0.57**	**0.40**	**0.70**	**0.64**
CNRM-CM5	**0.23**	**0.24**	**0.53**	**0.41**	**−0.21**	**−0.25**	**0.63**	**0.52**	−0.02	−0.08
CSIRO-Mk3.6.0	**0.31**	**0.33**	**0.66**	**0.56**	**−0.51**	**−0.52**	**0.78**	**0.64**	0.06	−0.01
GFDL-CM3	0.41	0.27	**0.65**	**0.83**	−0.25	**−0.54**	**0.50**	**0.57**	0.04	0.32
GISS-E2-H	**0.42**	**0.31**	**0.60**	**0.53**	**−0.42**	**−0.43**	**0.45**	**0.39**	**0.42**	**0.35**
GISS-E2-R	**0.36**	**0.38**	**0.63**	**0.59**	**−0.42**	**−0.37**	**0.56**	**0.55**	**0.29**	**0.36**
HadGEM2-ES	**0.52**	**0.48**	**0.67**	**0.64**	**−0.45**	**−0.35**	**0.73**	**0.64**	**0.19**	0.01
IPSL-CM5A-LR	**0.42**	**0.15**	**0.61**	**0.61**	**−0.35**	**−0.44**	**−0.26**	**0.61**	**0.59**	**0.39**
IPSL-CM5A-MR	0.11	0.02	**0.57**	**0.52**	**−0.34**	**−0.49**	**0.36**	**0.42**	**0.45**	**0.21**
MIROC-ESM	0.21	**0.28**	**0.83**	**0.65**	**−0.25**	−0.15	**0.81**	**0.76**	0.08	0.09
MRI-CGCM3	**0.34**	**0.27**	**0.50**	**0.48**	**−0.56**	**−0.42**	**0.57**	**0.61**	−0.01	−0.17
NorESM1-M	**0.40**	**0.37**	**0.56**	**0.54**	**−0.28**	**−0.36**	**0.49**	**0.52**	**0.57**	**0.60**

Where there are significant nonlinearities across the model ensemble in the local temperature response to global warming, it appears that other forcings than greenhouse gas emissions are likely to be at play. For the case study region of East Asia during boreal summer we identified that the departure from scaling at 2°C was associated with changes in the aerosol concentrations, due to anthropogenic emissions. In East Asia, whether a nonlinear local warming occurs will depend largely on changes in anthropogenic aerosol emissions. The increased local warming rate in East Asia from 1.5° to 2°C of global warming is seen in different RCP scenarios, consistent with the projected reduction in anthropogenic aerosol emissions (Lamarque et al. 2011), but the strength of the effect varies substantially due to natural variability superimposed on the nonlinear forced warming trend. While a reduction in the emission of aerosols would have direct benefits with regards to human health (Highwood and Kinnersley 2006), an unintended consequence could be increased summer temperatures arising from greater shortwave downwelling radiation at the surface. This has the unfortunate effect of not only increasing mean summer temperatures in the region, but also affecting climate extremes. The warming departure from scaling *very likely* (greater than 90% confidence) increases the occurrence of extreme hot summers over the region in the simulated 2°C world relative to the scaled 2°C world.

There is a range of climate model responses in terms of the deviation from scaling over East Asia. The models with the greatest exceedance of a scaled response at 2°C of global warming (i.e., the largest deviation) have the largest associated change in climate toward some synoptic conditions associated with heatwaves in the region (Freychet et al. 2017). The models for which East Asian summer temperatures most strongly exceed a scaled response tend to have the largest associated increases in 500-hPa geopotential height and 850-hPa specific humidity over the region and the greatest reduction in mean sea level pressure to the northeast of the region. Previous analysis has found increases in extreme rainfall metrics in the East Asia region using the Community Earth System Model and a degree of scenario dependence (Wang et al. 2017) to these increases. This study finds a projected increase in precipitation in the region (Fig. 8). We do not find an increase in extreme rainfall (Rx1day) over East Asia between 1.5° and 2°C of global warming (not shown); however, there are few models available for this analysis and there is a lack of agreement. We do not examine scenario dependence due to the small sample sizes of model years.

Our results over East Asia, in combination with the analysis of Wang et al. (2017), highlight the need to consider non–greenhouse gas forcings when investigating changes in local climate between the 1.5° and 2°C levels of global warming. On likely ''real-world'' pathways to 2°C, and under all RCPs, there would be an associated aerosol reduction causing an increase in likelihood of hot summers in the region.

Our analysis advances understanding of whether scaling regional warming as a function of global

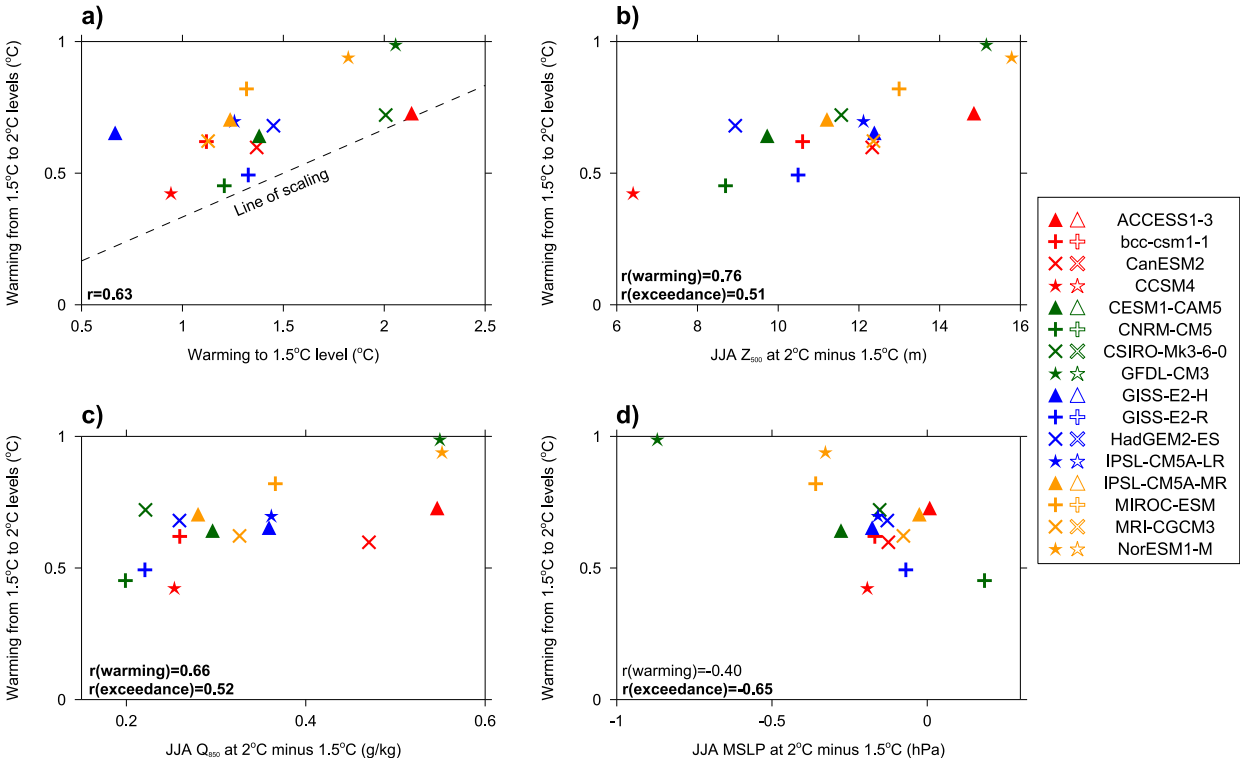

FIG. 12. (a) Scatterplot of model-simulated mean-average East Asian summer temperature warming to 1.5°C against mean-average summer warming from 1.5° to 2°C. The dashed line represents a scaled response. Also shown are scatterplots of model-simulated mean change in JJA average (b) 500-hPa geopotential height, (c) 850-hPa specific humidity, and (d) mean sea level pressure from 1.5° to 2°C global warming against the model-simulated mean warming from 1.5° to 2°C. Spearman rank correlations are shown between the change in the model mean of each atmospheric variable and both the warming from 1.5° to 2°C and the exceedance of scaling. These values are shown in bold where p values are below 0.05.

temperatures is a reasonable approach. However, more work toward evaluating scaling using other model experiments, such as in HAPPI (''half a degree additional warming, prognosis and projected impacts''; Mitchell et al. 2017, 2016b), and for temperature extremes, such as the hottest day of the year, would be of great use. Recent analysis based on the community climate simulations (Sanderson et al. 2017) and CMIP5, and using a different approach to this analysis, suggests that low warming scenarios can be approximated based on scaling from higher emissions projections due to the linearity of the climate response (Tebaldi and Knutti 2018).

In summary, our results based on individual models highlight the possibility of nonlinear temperature changes, but for most locations there is no systematic nonlinearity across the ensemble. In East Asia, where the warming does not simply ''scale up'' across the model ensemble, there are other influences than greenhouse gas concentrations that are taking effect. We highlight this issue through studying the effect of projected reductions in anthropogenic aerosol emissions over East Asia causing an increase in summer temperatures and raising the likelihood of extreme hot summers. This analysis illustrates that the occurrence of nonlinear local warming in response to global warming is largely related to changes in anthropogenic aerosols, which have large local-scale effects, as opposed to greenhouse gas emissions, which are well mixed and tend to have hemispheric and global effects instead.

Acknowledgments. We thank Daithi Stone and David Karoly for commenting on the manuscript prior to submission. Andrew King and Julie Arblaster were supported by the ARC Centre of Excellence for Climate Extremes (Grant CE170100023). Andrew King was also supported by the Australian Research Council (Grant DE180100638). Sophie Lewis was supported by the Australian Research Council (Grant DE160100092). Portions of this study were supported by the Regional and Global Climate Modeling Program (RGCM) of the U.S. Department of Energy's Office of Biological and Environmental Research (BER) Cooperative Agreement DE-FC02-97ER62402 and the National Science Foundation. We thank the NCI National Facility in

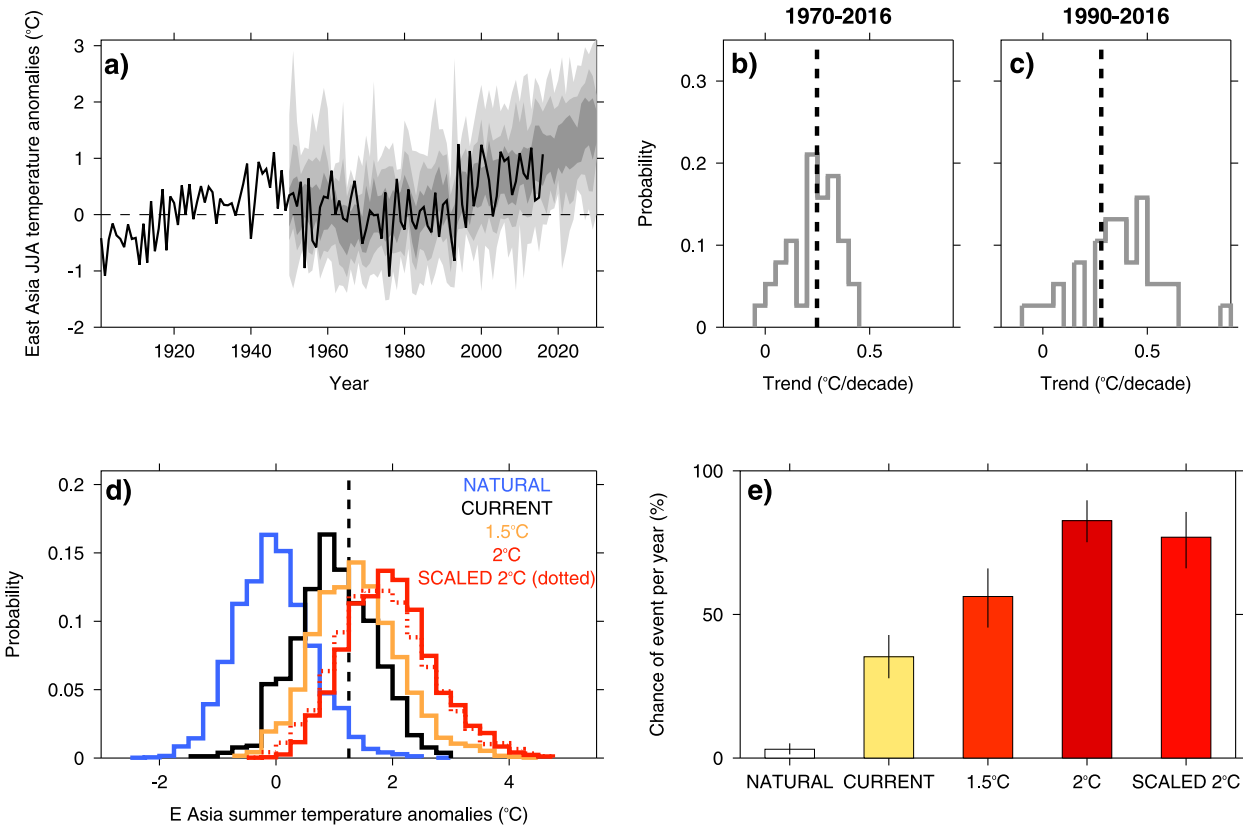

FIG. 13. (a) Time series of observed (black) and the full envelope (light gray), 5th–95th percentile range (gray), and interquartile range (dark gray) of model-simulated East Asian summer temperature anomalies. (b),(c) Observed (black dashed) and the distribution of model-simulated (gray) East Asian summer temperature trends for 1970–2016 and 1990–2016, respectively. (d) Probability distributions of East Asian summer temperature anomalies under the four principal scenarios, natural (blue), current (black), 1.5°C (orange), and 2°C (red), as well as the scaled 2°C scenario (dotted red). (e) The changing likelihood of record hot East Asian summers under natural, current, 1.5°, and 2°C conditions. Estimates for scaled a 2°C world are also shown. Best estimate likelihoods (calculated using the entire model ensembles representing each world) are displayed with 90% confidence intervals (derived from bootstrapping model subensembles) represented by the vertical black lines.

Australia for providing computing support and access to the CMIP5 and ERA-Interim data. We acknowledge the World Climate Research Program's Working Group on Coupled Modelling, which is responsible for CMIP, and we thank the climate modelling groups for producing and making available their model output.

REFERENCES

Arblaster, J. M., and G. A. Meehl, 2006: Contributions of external forcings to southern annular mode trends. *J. Climate*, **19**, 2896–2905, https://doi.org/10.1175/JCLI3774.1.

Collins, M., and Coauthors, 2013: Long-term climate change: Projections, commitments and irreversibility. *Climate Change 2013: The Physical Science Basis*, T. F. Stocker et al., Eds., 1029–1136, http://www.climatechange2013.org/images/report/WG1AR5_Chapter12_FINAL.pdf.

Dee, D. P., and Coauthors, 2011: The ERA-Interim reanalysis: Configuration and performance of the data assimilation system. *Quart. J. Roy. Meteor. Soc.*, **137**, 553–597, https://doi.org/10.1002/qj.828.

Deser, C., A. Phillips, V. Bourdette, and H. Teng, 2012: Uncertainty in climate change projections: The role of internal variability. *Climate Dyn.*, **38**, 527–546, https://doi.org/10.1007/s00382-010-0977-x.

Dosio, A., and E. M. Fischer, 2018: Will half a degree make a difference? Robust projections of indices of mean and extreme climate in Europe under 1.5°C, 2°C, and 3°C global warming. *Geophys. Res. Lett.*, **45**, 935–944, https://doi.org/10.1002/2017GL076222.

Eyring, V., and Coauthors, 2013: Long-term ozone changes and associated climate impacts in CMIP5 simulations. *J. Geophys. Res. Atmos.*, **118**, 5029–5060, https://doi.org/10.1002/jgrd.50316.

Freychet, N., S. Tett, J. Wang, and G. Hegerl, 2017: Summer heat waves over eastern China: Dynamical processes and trend attribution. *Environ. Res. Lett.*, **12**, 024015, https://doi.org/10.1088/1748-9326/aa5ba3.

Gillett, N. P., and P. A. Stott, 2009: Attribution of anthropogenic influence on seasonal sea level pressure. *Geophys. Res. Lett.*, **36**, L23709, https://doi.org/10.1029/2009GL041269.

Giorgi, F., and X. Bi, 2009: Time of emergence (TOE) of GHG-forced precipitation change hot-spots. *Geophys. Res. Lett.*, **36**, L06709, https://doi.org/10.1029/2009GL037593.

Good, P., and Coauthors, 2015: Nonlinear regional warming with increasing CO_2 concentrations. *Nat. Climate Change*, **5**, 138–142, https://doi.org/10.1038/nclimate2498.

——, B. B. B. Booth, R. Chadwick, E. Hawkins, A. Jonko, and J. A. Lowe, 2016: Large differences in regional precipitation change between a first and second 2 K of global warming. *Nat. Commun.*, **7**, 13667, https://doi.org/10.1038/ncomms13667.

Harris, I., P. D. Jones, T. J. Osborn, and D. H. Lister, 2014: Updated high-resolution grids of monthly climatic observations—The CRU TS3.10 dataset. *Int. J. Climatol.*, **34**, 623–642, https://doi.org/10.1002/joc.3711.

Hawkins, E., and R. Sutton, 2009: The potential to narrow uncertainty in regional climate predictions. *Bull. Amer. Meteor. Soc.*, **90**, 1095–1107, https://doi.org/10.1175/2009BAMS2607.1.

Held, I. M., and B. J. Soden, 2006: Robust responses of the hydrological cycle to global warming. *J. Climate*, **19**, 5686–5699, https://doi.org/10.1175/JCLI3990.1.

Herger, N., B. M. Sanderson, and R. Knutti, 2015: Improved pattern scaling approaches for the use in climate impact studies. *Geophys. Res. Lett.*, **42**, 3486–3494, https://doi.org/10.1002/2015GL063569.

Highwood, E. J., and R. P. Kinnersley, 2006: When smoke gets in our eyes: The multiple impacts of atmospheric black carbon on climate, air quality and health. *Environ. Int.*, **32**, 560–566, https://doi.org/10.1016/j.envint.2005.12.003.

Hurtt, G. C., and Coauthors, 2011: Harmonization of land-use scenarios for the period 1500–2100: 600 years of global gridded annual land-use transitions, wood harvest, and resulting secondary lands. *Climatic Change*, **109**, 117–161, https://doi.org/10.1007/s10584-011-0153-2.

James, R., R. Washington, C.-F. Schleussner, J. Rogelj, and D. Conway, 2017: Characterizing half-a-degree difference: A review of methods for identifying regional climate responses to global warming targets. *Wiley Interdiscip. Rev.: Climate Change*, **8**, e457, https://doi.org/10.1002/wcc.457.

King, A. D., and D. Karoly, 2017: Climate extremes in Europe at 1.5 and 2 degrees of global warming. *Environ. Res. Lett.*, **12**, 114031, https://doi.org/10.1088/1748-9326/aa8e2c.

——, and Coauthors, 2015a: The timing of anthropogenic emergence in simulated climate extremes. *Environ. Res. Lett.*, **10**, 094015, https://doi.org/10.1088/1748-9326/10/9/094015.

——, G. J. van Oldenborgh, D. J. Karoly, S. C. Lewis, and H. Cullen, 2015b: Attribution of the record high central England temperature of 2014 to anthropogenic influences. *Environ. Res. Lett.*, **10**, 054002, https://doi.org/10.1088/1748-9326/10/5/054002.

——, D. J. Karoly, and B. J. Henley, 2017: Australian climate extremes at 1.5°C and 2°C of global warming. *Nat. Climate Change*, **7**, 412–416, https://doi.org/10.1038/nclimate3296.

Kirtman, B., and Coauthors, 2013: Near-term climate change: Projections and predictability. *Climate Change 2013: The Physical Science Basis*, T. F. Stocker et al., Eds., Cambridge University Press, 953–1028, https://www.ipcc.ch/pdf/assessment-report/ar5/wg1/WG1AR5_Chapter11_FINAL.pdf.

Knutti, R., J. Rogelj, J. Sedláček, and E. M. Fischer, 2016: A scientific critique of the two-degree climate change target. *Nat. Geosci.*, **9**, 13–18, https://doi.org/10.1038/ngeo2595.

Kushner, P. J., I. M. Held, T. L. Delworth, P. J. Kushner, I. M. Held, and T. L. Delworth, 2001: Southern Hemisphere atmospheric circulation response to global warming. *J. Climate*, **14**, 2238–2249, https://doi.org/10.1175/1520-0442(2001)014<0001:SHACRT>2.0.CO;2.

Lamarque, J.-F., G. P. Kyle, M. Meinshausen, K. Riahi, S. J. Smith, D. P. van Vuuren, A. J. Conley, and F. Vitt, 2011: Global and regional evolution of short-lived radiatively-active gases and aerosols in the representative concentration pathways. *Climatic Change*, **109**, 191–212, https://doi.org/10.1007/s10584-011-0155-0.

Lehner, F., S. Coats, T. F. Stocker, A. G. Pendergrass, B. M. Sanderson, C. C. Raible, and J. E. Smerdon, 2017: Projected drought risk in 1.5°C and 2°C warmer climates. *Geophys. Res. Lett.*, **44**, 7419–7428, https://doi.org/10.1002/2017GL074117.

Lewis, S. C., and D. J. Karoly, 2013: Anthropogenic contributions to Australia's record summer temperatures of 2013. *Geophys. Res. Lett.*, **40**, 3705–3709, https://doi.org/10.1002/grl.50673.

——, and A. D. King, 2017: Evolution of mean, variance and extremes in 21st century temperatures. *Wea. Climate Extremes*, **15**, 1–10, https://doi.org/10.1016/j.wace.2016.11.002.

Ma, S., T. Zhou, D. A. Stone, O. Angélil, and H. Shiogama, 2017: Attribution of the July–August 2013 heat event in central and eastern China to anthropogenic greenhouse gas emissions. *Environ. Res. Lett.*, **12**, 054020, https://doi.org/10.1088/1748-9326/aa69d2.

Menary, M. B., and R. A. Wood, 2018: An anatomy of the projected North Atlantic warming hole in CMIP5 models. *Climate Dyn.*, **50**, 3063–3080, https://doi.org/10.1007/s00382-017-3793-8.

Min, S.-K., X. Zhang, F. W. Zwiers, and G. C. Hegerl, 2011: Human contribution to more-intense precipitation extremes. *Nature*, **470**, 378–381, https://doi.org/10.1038/nature09763.

Mitchell, D., and Coauthors, 2016a: Attributing human mortality during extreme heat waves to anthropogenic climate change. *Environ. Res. Lett.*, **11**, 074006, https://doi.org/10.1088/1748-9326/11/7/074006.

——, R. James, P. M. Forster, R. A. Betts, H. Shiogama, and M. Allen, 2016b: Realizing the impacts of a 1.5°C warmer world. *Nat. Climate Change*, **6**, 735–737, https://doi.org/10.1038/nclimate3055.

——, and Coauthors, 2017: Half a degree additional warming, prognosis and projected impacts (HAPPI): Background and experimental design. *Geosci. Model Dev.*, **10**, 571–583, https://doi.org/10.5194/gmd-10-571-2017.

Sanderson, B. M., and Coauthors, 2017: Community climate simulations to assess avoided impacts in 1.5°C and 2°C futures. *Earth Syst. Dyn.*, **8**, 827–847, https://doi.org/10.5194/esd-8-827-2017.

Schleussner, C.-F., and Coauthors, 2016: Differential climate impacts for policy-relevant limits to global warming: The case of 1.5°C and 2°C. *Earth Syst. Dyn.*, **7**, 327–351, https://doi.org/10.5194/esd-7-327-2016.

Seneviratne, S. I., M. G. Donat, A. J. Pitman, R. Knutti, and R. L. Wilby, 2016: Allowable CO_2 emissions based on regional and impact-related climate targets. *Nature*, **529**, 477–483, https://doi.org/10.1038/nature16542.

Sun, Q., C. Miao, A. AghaKouchak, and Q. Duan, 2017: Unraveling anthropogenic influence on the changing risk of heat waves in China. *Geophys. Res. Lett.*, **44**, 5078–5085, https://doi.org/10.1002/2017GL073531.

Sun, Y., X. Zhang, F. W. Zwiers, L. Song, H. Wan, T. Hu, H. Yin, and G. Ren, 2014: Rapid increase in the risk of extreme summer heat in eastern China. *Nat. Climate Change*, **4**, 1082–1085, https://doi.org/10.1038/nclimate2410.

Taylor, K. E., R. J. Stouffer, and G. A. Meehl, 2012: An overview of CMIP5 and the experiment design. *Bull. Amer. Meteor. Soc.*, **93**, 485–498, https://doi.org/10.1175/BAMS-D-11-00094.1.

Tebaldi, C., and J. M. Arblaster, 2014: Pattern scaling: Its strengths and limitations, and an update on the latest model simulations. *Climatic Change*, **122**, 459–471, https://doi.org/10.1007/s10584-013-1032-9.

——, and R. Knutti, 2018: Evaluating the accuracy of climate change pattern emulation for low warming targets. *Environ. Res. Lett.*, **13**, 055006, https://doi.org/10.1088/1748-9326/aabef2.

UNFCCC, 2015: Report on the structured expert dialogue on the 2013–2015 review. Rep. FCCC/SB/2015/INF.1, U.N. Framework Convention on Climate Change, 182 pp., https://unfccc.int/resource/docs/2015/sb/eng/inf01.pdf.

van Vuuren, D. P., and Coauthors, 2011: The representative concentration pathways: An overview. *Climatic Change*, **109**, 5–31, https://doi.org/10.1007/s10584-011-0148-z.

Wang, Z., L. Lin, X. Zhang, H. Zhang, L. Liu, and Y. Xu, 2017: Scenario dependence of future changes in climate extremes under 1.5°C and 2°C global warming. *Sci. Rep.*, **7**, 46432, https://doi.org/10.1038/srep46432.

Xu, Y., J.-F. Lamarque, and B. M. Sanderson, 2018: The importance of aerosol scenarios in projections of future heat extremes. *Climatic Change*, **146**, 393–406, https://doi.org/10.1007/s10584-015-1565-1.

Zhang, L., and C. Wang, 2013: Multidecadal North Atlantic sea surface temperature and Atlantic meridional overturning circulation variability in CMIP5 historical simulations. *J. Geophys. Res. Oceans*, **118**, 5772–5791, https://doi.org/10.1002/jgrc.20390.